

See discussions, stats, and author profiles for this publication at: <https://www.researchgate.net/publication/259718935>

Amphiphilic Drug-like Molecules Accumulate in A Membrane Below the Head Group Region.

ARTICLE in THE JOURNAL OF PHYSICAL CHEMISTRY B · JANUARY 2014

Impact Factor: 3.3 · DOI: 10.1021/jp4112052 · Source: PubMed

CITATIONS

14

READS

50

5 AUTHORS, INCLUDING:



Russell Devane

Procter & Gamble

50 PUBLICATIONS 1,283 CITATIONS

SEE PROFILE



Bruce Murch

Procter & Gamble

17 PUBLICATIONS 412 CITATIONS

SEE PROFILE



Karel Berka

Palacký University of Olomouc

49 PUBLICATIONS 674 CITATIONS

SEE PROFILE



Michal Otyepka

Palacký University of Olomouc

180 PUBLICATIONS 4,557 CITATIONS

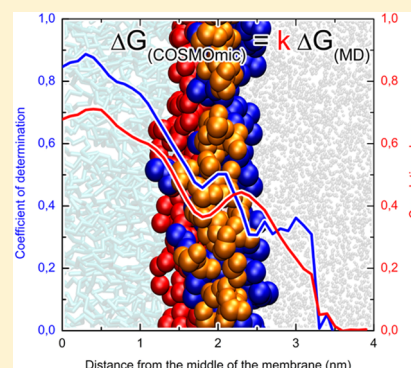
SEE PROFILE

Amphiphilic Drug-Like Molecules Accumulate in a Membrane below the Head Group Region

Markéta Paloncýová,[†] Russell DeVane,[‡] Bruce Murch,[‡] Karel Berka,^{*,†} and Michal Otyepka^{*,†}[†]Department of Physical Chemistry, Faculty of Science, Regional Centre of Advanced Technologies and Materials, Palacký University Olomouc, tř. 17. listopadu 12, 771 46 Olomouc, Czech Republic[‡]Corporate Modeling & Simulation, Procter & Gamble, 8611 Beckett Road, West Chester, Ohio 45069, United States

S Supporting Information

ABSTRACT: The partitioning behavior of drug-like molecules into biomembranes has a crucial impact on the design and efficacy of therapeutic drugs. Thermodynamic properties connected with the interaction of molecules with membranes can be evaluated by calculating free-energy profiles normal to the membrane surface. We calculated the free-energy profiles of 25 drug-like molecules in a 1,2-dioleoyl-*sn*-glycero-3-phosphocholine (DOPC) membrane and free energies of solvation in water and heptane using two methods, molecular dynamics (MD) simulations with the Berger lipid force field and COSMOmic, based on a continuum conductor-like screening model for realistic solvation (COSMO-RS). The biased MD simulations (in total $\sim 22 \mu\text{s}$ long) were relatively computationally expensive, whereas the COSMOmic approach offered a significantly less expensive alternative. Both methods provided similar results and showed that the studied amphiphilic drug-like molecules accumulate in the membrane, with the majority localized below the head group region. The MD simulations were more lipophilic and gave free-energy profiles that were systematically deeper than those calculated by COSMOmic. To investigate the physical nature of the increased lipophilicity, we analyzed a water/heptane system and identified that it is most likely caused by overestimation of the attractive term of the Lennard-Jones potential in lipid tails. We concluded that COSMOmic can be successfully used for high-throughput computations of global thermodynamic properties, for example, partition coefficients and energy barrier heights, in phosphocholine membranes. In contrast, MD is better for investigating local properties like molecular positioning and orientation in the membrane because they more accurately reflect the complex structure of lipid bilayers. MD is also useful for studies of highly complex systems, for example, drug–membrane–protein interactions.



INTRODUCTION

Molecular insight into the interactions of drugs (generally any xenobiotic) with biomembranes broadens our understanding of drug disposition in the human body and, in turn, absorption, distribution, metabolism, and excretion (ADME) processes. Absorption is influenced by the ability of a drug to cross the skin (in the case of a transdermal pathway) or the intestine wall (oral pathway). The distribution depends on the penetration of the drug through cell membranes. Metabolism of the drug is affected by the position and concentration of the drug in the relevant membrane, whereas its excretion depends on the penetration properties of the resulting metabolites and possible accumulation of drugs or metabolites in tissues. As biomembranes form barriers between environments with different properties, the thermodynamic and kinetic properties of drugs interacting with membranes is of particular interest.^{1–8}

Several experimental techniques have been employed for estimating partition and penetration properties of drug-like molecules.^{9–11} Commonly used techniques for partition measurements include, among others, ultracentrifugation, solid phase microextraction, and equilibrium dialysis.¹² Caco2 cells and skin penetration¹³ measurements are commonly used

to estimate penetration rates. These experimental techniques allow estimation of penetration and partitioning properties and their dependence on concentration, temperature, pressure, and so forth. However, they do not provide a detailed molecular-level understanding of drug–membrane interactions.

A considerable effort has been invested in developing *in silico* methods that can assess partitioning and permeation of drugs in membranes.^{5,14–19} The partitioning of a drug in a membrane can be rationalized by a free-energy profile along the lipid bilayer normal. The free-energy profile can be reconstructed from biased molecular dynamics (MD) simulations, typically from constraint simulations, umbrella sampling, metadynamics, or flooding.^{4,20–22} It is worth noting that MD simulations can accurately describe the complex structure of a lipid bilayer^{23,24} and simultaneously enable fine space (atomic) and time (sub-picosecond) resolutions. In addition, MD simulations can be used for dynamical studies of even more complex systems, for example, drug–membrane–protein interactions.²⁵ On the

Received: November 14, 2013

Revised: January 12, 2014

Published: January 13, 2014

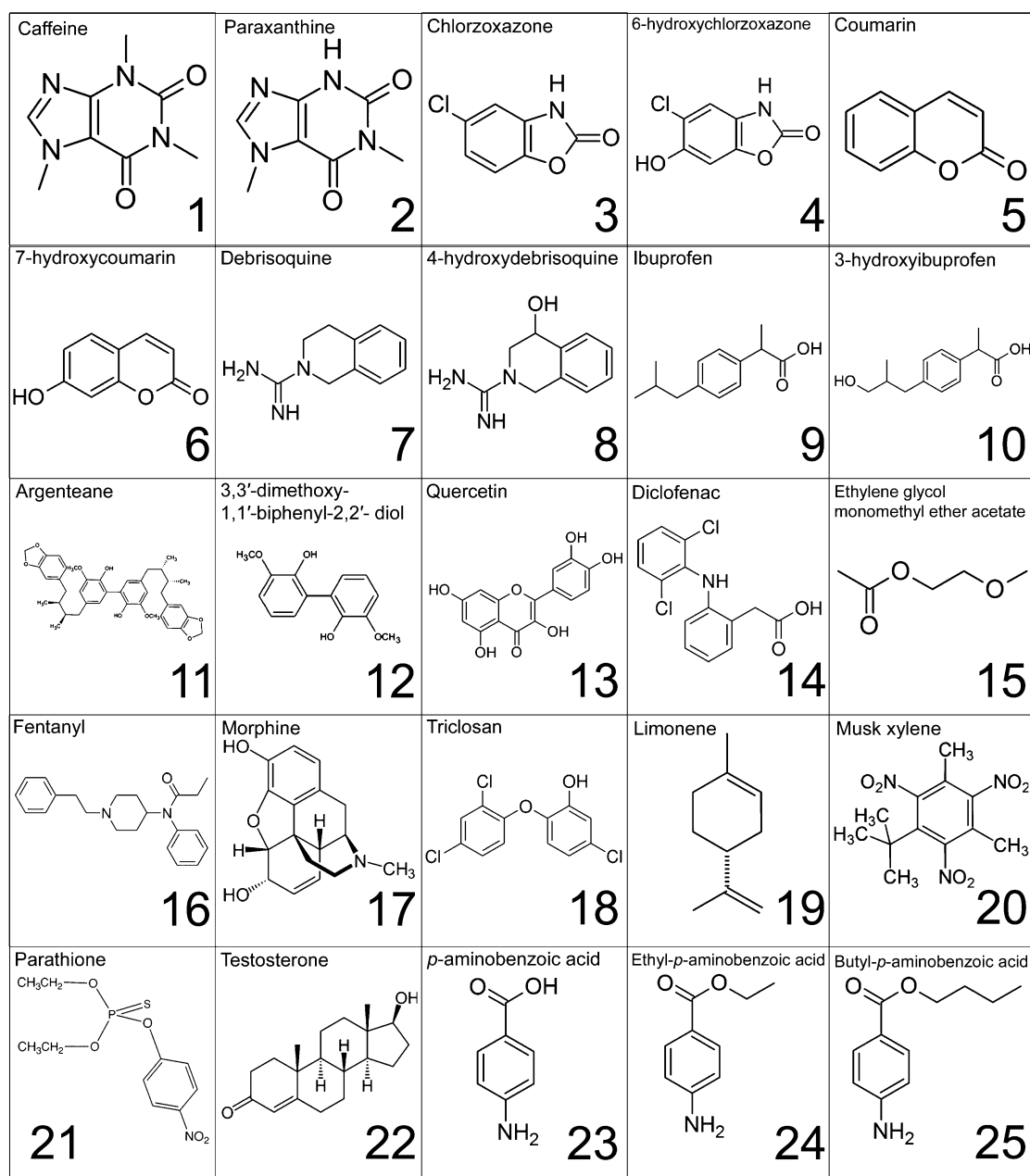


Figure 1. Structures and names of drugs used in this study. The numbers are consistent with the numbering in the rest of the paper.

other hand, the quality of MD simulations is highly dependent on the quality of the force field used (FF; an empirical potential or molecular mechanics potential).^{26–29} Recent studies have shown that the free-energy profiles of drugs on membranes display rather slow convergence,^{18,30} requiring long (typically 100+ ns) and consequently computationally demanding MD simulations. In addition, degrees of freedom other than just the distance from the membrane core need to be taken into account, which makes the calculation even more difficult.³¹ All of the above-mentioned features make MD simulations a powerful but expensive tool in the rationalization of drug partitioning properties.

The enormous computer demands required to obtain free-energy profiles from MD simulations has motivated many researchers to develop less expensive methods. Continuum solvation models based on quantum chemical calculations are a significantly less expensive and reliable alternative to MD

simulations.^{32,33} The COSMOmic approach³⁴ based on the COSMO-RS method³³ allows efficient and accurate prediction of the distribution of molecules in micellar systems and lipid bilayers.^{12,34,35} The COSMO-RS method applies statistical thermodynamics to surface polarization charge densities σ calculated from quantum chemical calculations, typically based on density functional theory (DFT). It has been shown that partition coefficients calculated by COSMOtherm into various homogeneous phases are in a good agreement with experimental data (with the average error of $\log K \approx 10\%$).³⁶ The COSMOmic method further analyzes the structure of a membrane in a solvent environment (water) and estimates the free-energy profile for a given molecule along the membrane normal. First, DFT calculations need to be performed for every molecule type in the system (lipids, water, drug molecules), and σ -profiles (histograms of charge densities σ) are obtained. Simply stated, the more complementary the σ -profiles of two

phases, the more miscible these phases. The following COSMOmic calculation is based only on analysis of geometries, rotation states, and σ -profiles of solute molecules and the membrane. The structure of a membrane is divided into layers, where each layer is considered as a separate fluid with its own σ -profile, which is calculated based on the parts of the molecular surface of each membrane molecular type present in each layer.³⁴ The center of mass of a molecule is placed into each layer, and by rotation of the solute, ~ 162 different directional representations are considered in each layer. For each state, COSMOmic calculates local σ -profiles (considering molecular segments in neighboring layers), which are then used to generate an integral σ -profile. This calculation is again based on the geometrical analysis of molecular orientation and identifies which part of the molecular surface is present in individual membrane layers. From this information, the overall solvation energy of the molecule in each layer is calculated, and the free-energy profile is constructed. The COSMOmic calculation is a relatively quick (it takes just a few minutes on a desktop computer but requires σ -profiles that are calculated within a few hours for considered molecules) and simple method to obtain the free-energy profile of a molecule in a membrane. However, to the best of our knowledge, no comparisons of COSMOmic to other computational approaches have been published.

In this work, we calculated the free-energy profiles of a set of 25 drug-like molecules (Figure 1) in a DOPC membrane and the solvation energies of those molecules in water and heptane. We used both MD simulations with the Berger lipid FF and COSMOmic. Both methods showed that the molecules accumulate in the membrane environment, with the majority lying just below the polar head group region. In the case of DOPC, we observed a significant correlation between the methods with regard to the height of the free-energy barrier between the water and lipid environment. There was also a strong correlation between the partition coefficients and partitioning into the hydrophobic part of the membrane. However, there were large differences in the details around the head group area, mainly in the location of the energy minimum and the energy barrier of crossing the membrane center. Some of these differences were attributed to the higher lipophilicity of the Berger lipid FF stemming from an overestimated Lennard-Jones term.

METHODS

The equilibrated DOPC membrane model²⁷ was downloaded from the Lipidbook web page³⁷ and was equilibrated for 10 ns using classical MD simulation at 310 K. The united-atom Berger lipid FF,³⁸ which simplifies hydrocarbon chains by uniting nonpolar hydrogens with the corresponding carbons, was applied to the lipid bilayer. The drugs were prepared by combining the PRODRG³⁹ tool and RESP^{40–43} calculation (see the Supporting Information). The drug molecules were placed at the top of the simulation box and hydrated with SPC or SPC/E water molecules (see the Supporting Information Table S1). Free-energy profiles, $\Delta G(z)$, were calculated either by umbrella sampling (eq 1), as described in our recent paper,⁴⁴ or by using our proposed simulation protocol³⁰ with z -constraint simulation (eq 2).

$$\Delta G(z) = -RT \ln P(z) + U(z) \quad (1)$$

$$\Delta G(z) = - \int_{\text{outside}}^{z'} \langle \vec{F}(z) \rangle_t dz \quad (2)$$

where $P(z)$ stands for the distribution of the studied molecule in the umbrella sampling simulation window, $U(z)$ stands for the umbrella potential, and $\langle \vec{F}(z) \rangle_t$ stands for the time-averaged force applied to the molecule during the z -constraint simulation. The start of the z -axis was set to the middle of the membrane, and the reference value ($\Delta G = 0$ kcal/mol) for the free energy was set to that for water. The detailed simulation protocol can be found in the Supporting Information. It is worth noting that the same simulation protocol has been successfully applied to study the penetration properties of various drugs and antioxidants.^{2,5,18,20,30,44,45}

For the COSMOmic calculations, we used a set of 30 structures taken from a 100 ns long MD simulation of a DOPC membrane to increase the precision of the calculations, as recommended in the literature.³⁵ The geometries and σ -profiles of all molecules were calculated by DFT/COSMO calculations at the BP/TZVP level of theory.^{46,47} Free-energy profiles were calculated at 310 K, with the membrane separated into 50 layers and 162 orientations of the solute molecules generated using COSMOmic software³⁴ from the COSMOtherm 13 package.⁴⁸ The free-energy profiles were averaged and compared to those obtained by MD.

The free-energy profiles provided information about (i) the position of the free-energy minimum, (ii) the height of the free-energy barriers (penetration barrier and water/lipids barrier – affinity to membrane), and (iii) the partition coefficient in the water/membrane environment. The overall distribution coefficient D of a molecule between membrane and water phases can be expressed in terms of the free energies in these phases (eq 3) and depends on the partition coefficient into membrane K , membrane surface S_{membrane} , and the volume of the water phase V_{water} . As the ratio of the membrane surface and water volume can be considered constant in the human body, we focus here just on the partition coefficient into membrane K that is reconstructed from the free-energy profile along the membrane (L nm thick) using eq 4

$$D = \frac{\iint_{\text{Surface}} dx dy \int_{-L/2}^{L/2} e^{-\Delta G(z)/RT} dz}{\iiint_{\text{Volume}} e^{-\Delta G(\text{water})/RT} dx dy dz} = \frac{S_{\text{membrane}}}{V_{\text{water}}} \cdot K \quad (3)$$

$$K = 2 \int_{L/2}^0 K(z') dz = 2 \int_{L/2}^0 e^{-\Delta G(z')/RT} dz \quad (4)$$

The free-energy profiles obtained by MD and COSMOmic were analyzed, and several parameters were compared (see Figure 2): (i) free-energy values at different membrane depths, $\Delta G(z)$, (ii) positions of the free-energy minima, Z_{min} , (iii) the local partition coefficient as a function of membrane depth, $K(z)$, (iv) the height of penetration barriers, ΔG^{pen} , and (v) the height of water/lipid barriers, ΔG^{wat} (lipophilicity and $\log K$).

Further, we calculated the transfer free energy from water to heptane $\Delta G^{\text{wat/heptane}}$ by COSMOtherm and MD. For the COSMOtherm calculations, we used the same molecular geometries and σ -profiles as described above for COSMOmic and default settings for the free energy of solvation calculation. The MD calculations utilized the thermodynamic integration method with the Bennett acceptance ratio (BAR).⁴⁹ A molecule of heptane was prepared to mimic the properties of a membrane core in the simulations. Therefore, the same charges

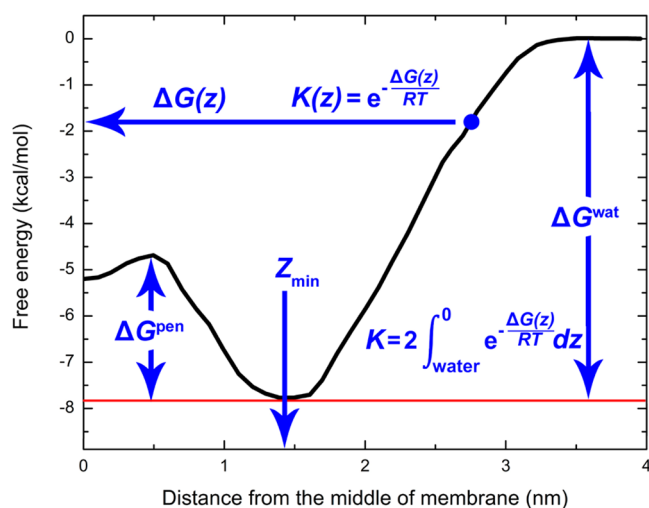


Figure 2. Prototypical free-energy profile of a drug along the bilayer normal showing the free energy $\Delta G(z)$ at different depths (z). $K(z)$ is the local partition coefficient at a distance z from the bilayer center, ΔG^{pen} is the free-energy barrier for penetration across the bilayer core, and z_{min} is the position of the free-energy minimum. ΔG^{wat} is the water/lipid barrier (affinity to the membrane), which makes the largest contribution to the overall partition coefficient K .

(assigned zero partial charges to all atoms) and atom types were used as those in the lipid tails in the Berger FF. An SPC/E⁵⁰ water model was used to calculate hydration free energies. Each drug molecule was placed in the simulation box and solvated with either water or heptane (~ 1.5 nm distance from drug to box edges). Then, the system was equilibrated for 100 ps. Twenty-one simulation windows ($\Delta\lambda = 0.05$) were run for 200 ps, and the last 100 ps was analyzed using g_{bar} from the GROMACS 4.5.1 software package. We evaluated the correlation of solvation free energies in water ΔG^{hyd} and heptane ΔG^{sol} by COSMOtherm and MD; we also evaluated $\Delta G^{\text{wat/heptane}}$ between the two methods and, last, compared $\Delta G^{\text{wat/heptane}}$ with the free energies in the middle of the membrane.

We plotted the free-energy profile parameters in DOPC in correlation plots and fitted the data to a straight line of the form $Y_{\text{COSMOmic}} = k(\text{err}) \cdot X_{\text{MD}} + q(\text{err})$, where k is the slope and q the intercept and their errors are in brackets. We evaluated the significance of the intercept parameter at a probability level of 0.975. In the case of a statistically insignificant intercept, we fitted the data to $Y_{\text{COSMOmic}} = k(\text{err}) \cdot X_{\text{MD}}$.

RESULTS AND DISCUSSION

We calculated free-energy profiles for 25 drug-like molecules in a DOPC membrane using biased MD simulations and COSMOmic. A typical free-energy profile of an amphiphilic molecule in a DOPC membrane calculated by MD is shown in Figure 2, and all free-energy profiles calculated in this study are shown in Figure S1 in the Supporting Information. Initially, the free energy decreased as the molecule approached the membrane surface from the water phase. Interestingly, the simulations predicted that some of the molecules have a small barrier to entry (approximately 1 kcal/mol) as they pass through the head group region (2.0–2.5 nm; all depths are reported as the distance from the membrane center). The free-energy minimum was usually located below the head groups (1.1–1.7 nm) and was 2–11 kcal/mol deep for most of the

molecules studied here. The free energy then increased until about 0.5 nm from the membrane center. In the membrane center, there was a shallow local energy minimum. In the case of lipophilic molecules, the free energy decreased to a minimum at the membrane center. The free-energy profiles calculated by COSMOmic displayed similar behavior in the outer parts of the membrane but had a different shape in the membrane interior. The free energies of lipophilic molecules reached an almost constant value at about 1.0 nm from the membrane center, whereas the amphiphilic molecules exhibited an almost constant free energy starting at approximately 0.5 nm from the bilayer center. Neither type of molecule displayed a local free-energy minimum at the membrane center. The free-energy minima calculated by COSMOmic were localized in two regions, at 0.7–1.5 and 2.0–2.6 nm.

Both methods, MD and COSMOmic, ranked the drug's affinity for the membrane in a comparable order, that is, water/lipid barrier ΔG^{wat} (Figure 3 and eq 5)

$$\Delta G_{\text{COSMOmic}}^{\text{wat}} = 0.62(0.08)\Delta G_{\text{MD}}^{\text{wat}} - 0.16(0.74)$$

$$r^2 = 0.73 \quad (5)$$

Linear regression analysis showed that COSMOmic predicted lower free-energy barriers (ΔG^{wat}) by about 40% but did not indicate any statistically significant shift. The coefficient of determination (which is equal to 1 in the case of strict linear dependence) was found to be $r^2 = 0.73$. The penetration barriers ΔG^{pen} predicted by COSMOmic were also about 40% lower than those predicted by MD, but the correlation between the two methods was lower, $r^2 = 0.59$ (eq 6)

$$\Delta G_{\text{COSMOmic}}^{\text{pen}} = 0.63(0.11)\Delta G_{\text{MD}}^{\text{pen}} + 0.13(0.65)$$

$$r^2 = 0.59 \quad (6)$$

The partition coefficients (Figure 3) calculated by both methods showed that all molecules included in this study tended to accumulate in the membrane. However, $\log K$ (eq 4) calculated by COSMOmic was almost 40% smaller than that by MD, but there was a significant linear relationship between the methods (eq 7)

$$\log K_{\text{COSMOmic}} = 0.63(0.07) \log K_{\text{MD}} - 0.01(0.47)$$

$$r^2 = 0.77 \quad (7)$$

These data indicate that drugs described by MD using the Berger lipid FF are more lipophilic than those obtained by COSMOmic. Previous COSMOmic $\log K$ calculations in 1,2-dimyristoyl-*sn*-glycero-3-phosphocholine (DMPC) have shown good correlation with experimentally measured $\log K$ (RMSE of $\log K$ from 0.34 to 0.79),^{12,14,35} with a coefficient of determination of linear fit to experimental data varying from 0.74 to 0.82.³⁴ Therefore, it is likely that COSMOmic would also show good performance for DOPC (DOPC and DMPC possess the same head groups but slightly different alkyl chains). Thus, the results indicate that MD simulations with the Berger lipid FF may systematically overestimate the real partition coefficients, drug affinities for a DOPC bilayer, and heights of penetration barriers (by $\sim 40\%$). Nonetheless, it is able to distinguish between low/high “membranophilic” drugs. This finding is also in agreement with observations by MacCallum et al.,⁵¹ who obtained correct ordering for the binding free energies of amino acids side chains to a POPC membrane.

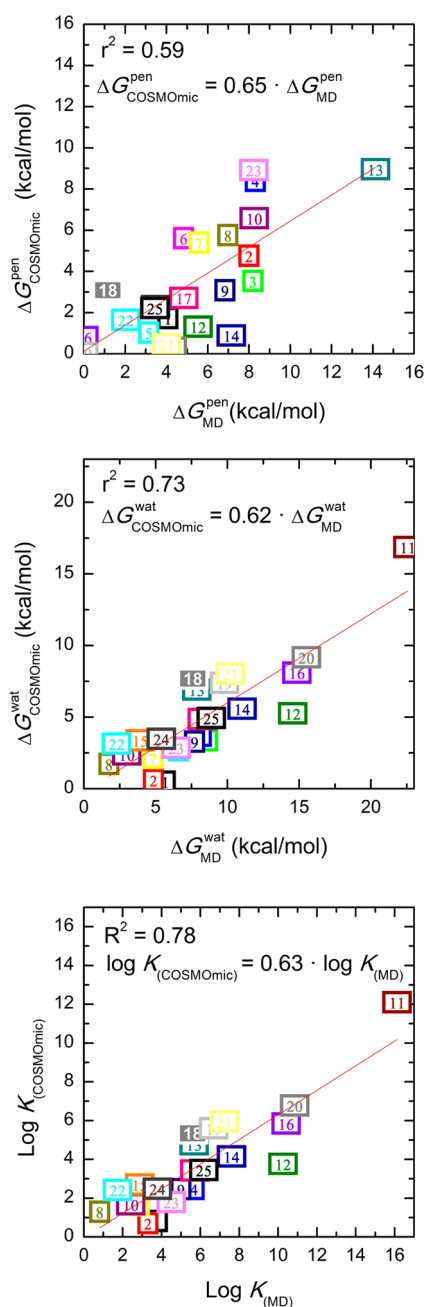


Figure 3. Comparison of the methods used showing the correlation of free-energy profile parameters calculated using COSMOmic (y-axis) and MD (x-axis). The penetration barrier (upper panel ΔG^{pen}) exhibited a relatively low coefficient of determination, r^2 , between the COSMOmic and MD values, whereas the water/lipid barrier (middle panel ΔG^{wat}) and partition coefficient (lower panel) correlated significantly. The numbers in the charts identify the molecules according to Table S1 (Supporting Information).

The structure of a lipid bilayer is rather complex⁵² (cf. Figure 4), and we anticipate that the local partitioning into different membrane depths by atomistic MD simulations may better reflect the membrane structure compared to the continuous-like model implemented in COSMOmic. The free energy of the drug ($\Delta G(z)$) at a given depth (z) and local partition coefficient ($K(z)$, eq 4) at the same depth calculated from the MD simulations mirrored the structure and density profile of the lipid bilayer. Peaks in the local partition coefficient

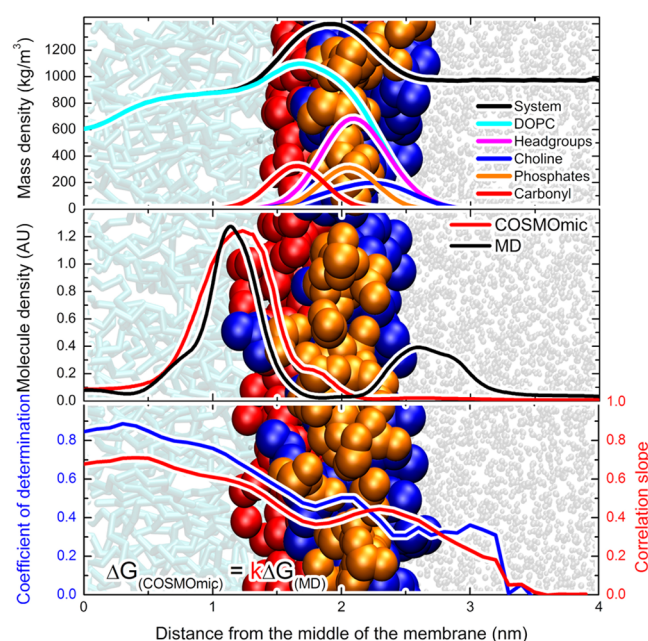


Figure 4. Background image showing the structure of a single leaflet of a hydrated lipid bilayer. Upper panel: mass densities of monitored groups. (Middle panel) Average mass density calculated from the local partition coefficients, $K(z)$, of drug molecules predicted by MD (black) and COSMOmic (red). The partition coefficient profiles were normalized and summed afterward. The MD partitioning favors specific locations in the membrane, whereas COSMOmic places all molecules into one broad region. (Lower panel) Coefficient of determination r^2 (blue) and slope (red) obtained from linear regression analysis of the z -dependent free-energy values between the COSMOmic and MD methods. A correlation slope lower than 1.0 indicates a shallower free-energy profile predicted by COSMOmic.

calculated by MD were found in three regions, (i) just below the head group region, where most of the drug molecules were localized, (ii) outside of the head group region at the interface with water, and (iii) in the middle of the membrane, which has the lowest density of lipids (Figure 4). The local partition coefficients predicted by COSMOmic were mostly localized to one broad area below the head group region. Unlike the MD calculations, COSMOmic showed almost constant partitioning into the region of the lipid tails (cf. Figure S1 (Supporting Information) and Figure 4), indicating that the position in the very middle of the membrane is not favored, as would be expected due to the decreased lipid density in that region. Similarly, MD predicted lower local partition coefficients than COSMOmic in the area of high membrane density (1.7–2.0 nm).

Neither COSMOmic nor MD favored the densest layer of the membrane as a free-energy minimum (Figure 5). However, the positions of the free-energy minima predicted by MD differed substantially from those by COSMOmic; the minima predicted by MD usually lay (i) in the lower parts of the head group region or just below it or (ii) in the middle of the membrane, where the overall density decreases. COSMOmic did not favor the energy minimum in the middle of the membrane and instead placed the molecules in a broad area in the outer parts of head groups (2.0–2.6 nm) or in the lipid tails below the head groups (0.7–1.5 nm). According to the positions of the free-energy minima, the molecules could be separated into three clusters, (i) lipophilic molecules that are localized in the middle of the membrane according to MD and

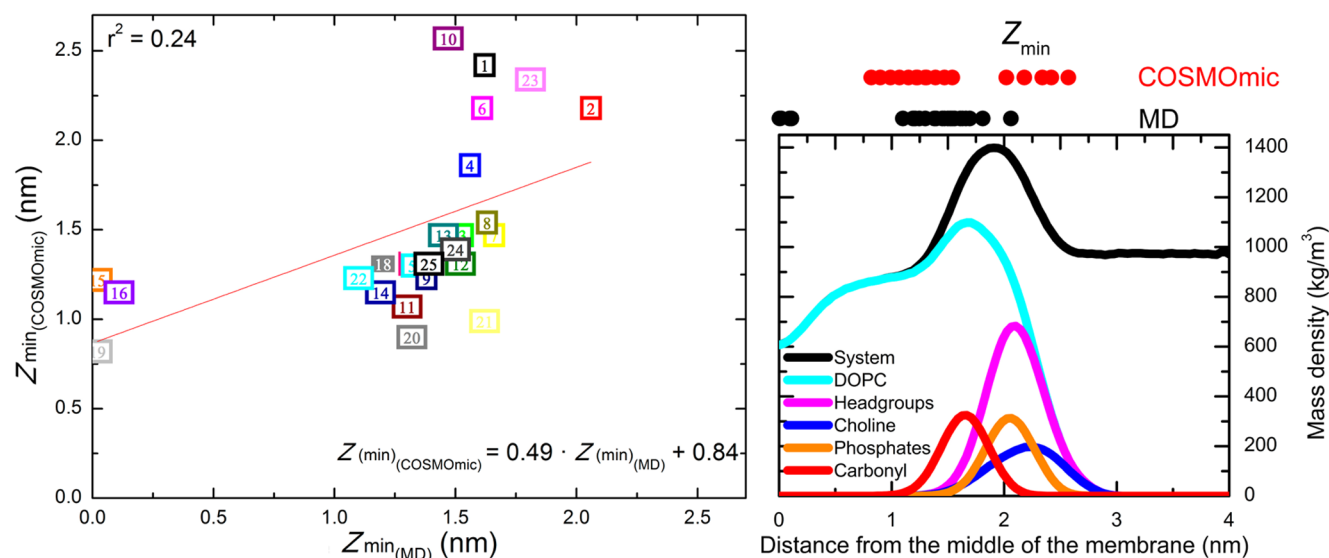


Figure 5. Positions of the free-energy minima Z_{\min} (left panel) proposed by COSMOmic (y-axis) and MD (x-axis) and compared to the system density (right panel). The minima predicted by MD were located in the lower part of the head groups or just below them or in the middle of the membrane (upper right panel, black circles). The minima predicted by COSMOmic were located above the head groups or in the lipid tail region (red circles).

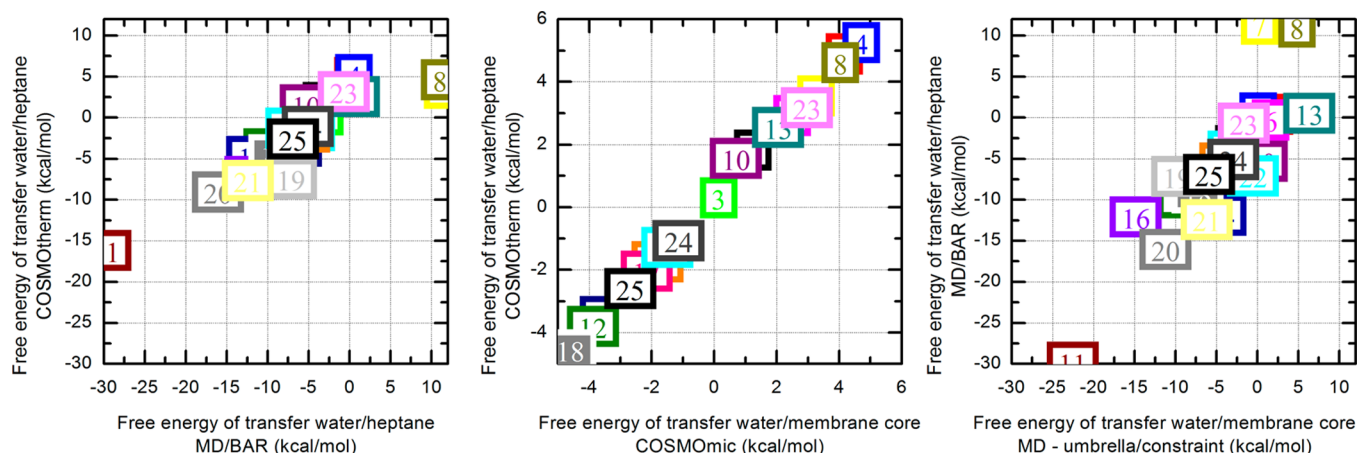


Figure 6. Correlation of the free energies of transfer from water to heptane $\Delta G^{\text{wat/heptane}}$ calculated by COSMOtherm and MD (left). Correlation of the free energies of transfer from water to heptane $\Delta G^{\text{wat/heptane}}$ and to the membrane core $\Delta G^{\text{wat/membrane core}}$ for COSMOtherm/COSMOmic (middle) and MD calculated with the Bennett acceptance ratio method (MD-BAR)/MD-umbrella/constraint (right).

around 1.0 nm according to COSMOmic (note again that ΔG^{pen} predicted by COSMOmic was very small), (ii) those localized below the head groups or in lower parts of the head groups according to both methods, and (iii) those localized in the lower parts of the head groups according to MD and at the outer part of head groups according to COSMOmic. It should be noted that the local partition coefficient, $K(z)$, discussed in the previous paragraph reflects both the overall free-energy profile shape (as each $K(z)$ profile was normalized) and also the average of all profiles. Therefore, the local partition coefficient outside of the membrane calculated by COSMOmic was very low even though there were some shallow free-energy minima in this region. The reliability of MD for predicting drug positioning in membranes has been shown in recent studies, where the positions of coumarin derivatives in a DMPC lipid bilayer predicted by MD with the Berger lipid FF³⁰ agreed well with positions determined by NMR.⁵³ The positions of fluorescent probes calculated by MD also agreed well with experimental observations.^{54,55} The molecular positions

suggested by MD seem to more sensitively reflect the local organization and density of the membrane regions than COSMOmic.

We analyzed the free-energy values at different membrane depths and observed an increasing correlation with decreasing distance to the membrane center (Figure 3). The slope, k , of the linear fit, $\Delta G_{\text{COSMOmic}} = k \cdot \Delta G_{\text{MD}}$, reached 0.7 in the membrane core and decreased toward the water phase. On the membrane surface (at 2.8 nm), the slope decreased to $k = 0.3$. The uncertainty (calculated as the percentage of the slope error with respect to the slope value) of the slope rapidly increased from 20% inside of the membrane to 100% in bulk water. The strongest correlation ($r^2 > 0.8$) of the free-energy values was found in the middle of the membrane and decreased toward the outer parts of the membrane. However, it was still statistically significant even at $\alpha = 0.001$. In other words, the free-energy profiles obtained by COSMOmic were shallower than those obtained by MD. However, both profiles could be derived from

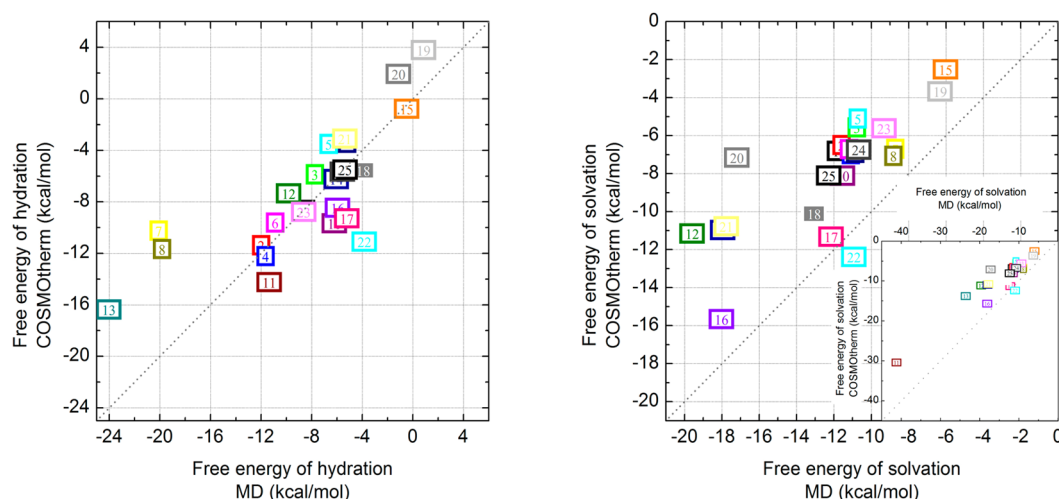


Figure 7. Free energies of solvation in water ΔG^{hyd} (left) and heptane ΔG^{solv} (right) calculated by COSMOtherm and MD. The hydration free energies (left) calculated by COSMOtherm and MD were in closer agreement than the corresponding solvation energies in heptane. The free energies of solvation in heptane were more negative by MD than COSMOtherm in all but one case.

each other with good precision because of the significant linearity.

The heterogeneity of membrane environments complicates direct comparison of free-energy profile properties, especially heights of free-energy barriers, to experimental results. However, such a comparison is straightforward for a binary system where the free energy of transfer between phases can be directly compared to the partition coefficient between the phases, as COSMOtherm has been shown to agree well with experimental partition coefficients.³⁶ The transfer free energies between water and heptane ($\Delta G^{\text{wat/heptane}}$) correlated well between the two methods (eq 8, Figure 6)

$$\Delta G_{\text{COSMOtherm}}^{\text{wat/heptane}} = 0.57(0.06)\Delta G_{\text{MD}}^{\text{wat/heptane}} + 1.42(0.54) \quad (8)$$

$$r^2 = 0.81$$

These data again show that MD with the Berger lipid FF leads to more lipophilic results, in agreement with the data acquired for MD of a DOPC membrane.

We might expect that the transfer free energies from water to heptane would tightly correlate with the transfer free energies between water and the membrane center.^{51,56} Given this assumption, we compared the transfer free energies from both methods. The fit of COSMOtherm $\Delta G^{\text{wat/heptane}}$ to the COSMOmic transfer free energies to the membrane core $\Delta G^{\text{wat/membrane}}$ (which literally corresponds to $\Delta G(0)$; see Figure 2) was almost perfect, explaining 99.7% of the data variability (eq 9)

$$\Delta G_{\text{COSMOtherm}}^{\text{wat/heptane}} = 1.04(0.01)\Delta G_{\text{COSMOmic}}^{\text{wat/membrane}} + 0.34(0.06) \quad (9)$$

$$r^2 = 0.997$$

$$\Delta G_{\text{MD}}^{\text{wat/heptane}} = 1.12(0.14)\Delta G_{\text{MD}}^{\text{wat/membrane}} - 1.09(1.02) \quad (10)$$

$$r^2 = 0.73$$

On the other hand, the fit of the MD data explained only 73% of the data variability (eq 10). Possible reasons for this are that the MD data may suffer from insufficient robust sampling and convergence issues^{18,30} or by solute-induced membrane perturbation. Another explanation is that larger molecules may be more affected by the complex membrane structure⁵² because they may reach from the nonpolar membrane core up

to the head groups (or up to the water). As, in principle, this would also affect the comparison of $\Delta G^{\text{wat/heptane(membrane)}}$ calculated by COSMOtherm and COSMOmic, for which we observed a tight correlation, we may conclude that this effect plays a negligible role.

To obtain a deeper understanding of the physical reasons for the higher lipophilicity of MD simulations, we analyzed the solvation free energies of drugs in water (ΔG^{hyd}) and heptane (ΔG^{solv}) and compared the mean errors in the COSMOtherm and MD values (Table S3 (Supporting Information) and Figure 7). Comparison of the hydration free energies ΔG^{hyd} calculated by COSMOtherm to those calculated by MD revealed a mean difference of -0.86 kcal/mol (mean absolute difference of 2.74 kcal/mol), whereas for ΔG^{solv} , the mean difference was -4.64 kcal/mol (mean absolute difference of 4.76 kcal/mol). These results indicate that ΔG^{hyd} was comparable for the two methods, but ΔG^{solv} was systematically predicted to be 30% lower by MD, that is, more lipophilic, than that by COSMOtherm (Figure 7) as the linear fit to the data (eq 11) was

$$\Delta G_{\text{COSMOtherm}}^{\text{solv}} = 0.71(0.06)\Delta G_{\text{MD}}^{\text{solv}} + 0.66(0.93) \quad (11)$$

$$r^2 = 0.85$$

where the intercept is statistically insignificant from 0 (at $\alpha = 0.05$).

We modeled partitioning between water and heptane phases to rationalize the differences observed for water–membrane partitioning estimated from MD and COSMOtherm. Such a simplified model enabled comparison of the transfer free energies between water and heptane phases and enumeration of solvation free energies in each phase. This provided a deeper physical–chemical insight into the interaction of solutes with both phases. ΔG^{hyd} calculated by COSMOtherm and MD were biased by lower errors than ΔG^{solv} , which was about 30% more lipophilic according to the MD simulations. In the united atom Berger lipid FF, no charges are present on lipid tails (the same applies for the heptane model used). Therefore, all interactions between the lipid tails or heptane and a drug molecule must originate from the Lennard-Jones term. Taking COSMOtherm data as reference values (as they have been shown to fit the experimental data well³⁶ and partitioning into a homogeneous

phase usually matches experiment), we concluded that combination of the Berger lipid FF with the GROMOS 53a6 FF⁵⁷ (where Lennard-Jones parameters are used to describe interactions of nonlipid atoms of drug-like molecules) leads to overestimation of the attractive term of the Lennard-Jones potential, which in turn overestimates partitioning into lipids. This finding may also help further adjustment of the Berger-like FF.

CONCLUSION

We calculated the free-energy profiles of 25 drug-like amphiphilic molecules in a DOPC lipid bilayer using both MD with the Berger lipid FF and COSMOmic. Solvation free energies of these molecules were also calculated in water and heptane. The calculated free-energy profiles and derived thermodynamic parameters were in good agreement between the two methods. All molecules used in this study were found to accumulate in the membrane, and most localized below the lipid head groups. Detailed analysis of the free-energy profiles in DOPC showed that the MD simulations more sensitively reflected the structural properties of the lipid bilayer. Thus, MD simulations are proposed to be a reliable tool for estimating the membrane localization of drug-like molecules or for analyzing structural features of more complex systems containing, for example, lipids, drugs (antioxidants or other ligands), and proteins. We also showed that the global thermodynamic parameters of drugs on PC membranes (especially ΔG^{wat} and $\log K$) can be calculated by COSMOmic, which offers an inexpensive alternative to computationally demanding MD. By testing a less expensive model of a membrane core (the heptane phase), we identified the origin of the apparent increased lipophilicity of molecules studied by MD with the Berger lipid FF. As the united-atom Berger lipid FF has uncharged lipid tails, the overestimated lipophilicity was attributed to over-attractive Lennard-Jones interactions. Our results show that further studies of lipid FFs and their interactions with other molecules are needed as MD simulations remain the method of choice for dynamic studies of complex systems, such as protein–membrane interactions.

ASSOCIATED CONTENT

Supporting Information

Details of the simulation protocol. Table S1: Simulation protocols for all molecules examined in this study. Table S2: Free-energy profile parameters on DOPC calculated by MD and COSMOmic. Table S3: Free energies of hydration and solvation. Figure S1: Free-energy profiles of all molecules calculated in this study. Figure S2: Correlation plots of free-energy profile values. This material is available free of charge via the Internet at <http://pubs.acs.org>.

AUTHOR INFORMATION

Corresponding Authors

*E-mail: karel.berka@upol.cz. Tel: +420 585 634 756 (K.B.).

*E-mail: michal.otyepka@upol.cz. Tel: +420 585 634 756 (M.O.).

Notes

The authors declare no competing financial interest.

ACKNOWLEDGMENTS

This work was supported by the Operational Program Research and Development for Innovations - European Regional

Development Fund (CZ.1.05/2.1.00/03.0058) and European Social Fund (CZ.1.07/2.3.00/20.0017 and/20.0058). M.O. acknowledges support by the Czech Grant Agency through the P208/12/G016 project. K.B. acknowledges support by the Czech Grant Agency through the P303/12/P019 project. M.P. acknowledges support by the Student Project PrF 2013_028 (Palacký University, Olomouc). This research used resources of the Oak Ridge Leadership Computing Facility at the Oak Ridge National Laboratory, which is supported by the Office of Science of the U.S. Department of Energy under Contract No. DE-AC05-00OR22725. We thank Andreas Klamt for insightful comments concerning COSMOmic methodology.

REFERENCES

- (1) Peters, G. H.; Wang, C.; Cruys-Bagger, N.; Velardez, G. F.; Madsen, J. J.; Westh, P. Binding of Serotonin to Lipid Membranes. *J. Am. Chem. Soc.* **2013**, *135*, 2164–2171.
- (2) Podloucká, P.; Berka, K.; Fabre, G.; Palonciová, M.; Duroux, J.-L.; Otyepka, M.; Trouillas, P. Lipid Bilayer Membrane Affinity Rationalizes Inhibition of Lipid Peroxidation by a Natural Lignan Antioxidant. *J. Phys. Chem. B* **2013**, *117*, 5043–5049.
- (3) Berka, K.; Hendrychová, T.; Anzenbacher, P.; Otyepka, M. Membrane Position of Ibuprofen Agrees with Suggested Access Path Entrance to Cytochrome P450 2C9 Active Site. *J. Phys. Chem. A* **2011**, *115*, 11248–11255.
- (4) Orsi, M.; Essex, J. W. Passive Permeation Across Lipid Bilayers: A Literature Review. In *Molecular Simulations and Biomembranes*; Sansom, M. S. P., Biggin, P. C., Eds.; Royal Society of Chemistry: Cambridge, U.K., 2010; pp 76–90.
- (5) Orsi, M.; Essex, J. W. Permeability of Drugs and Hormones through a Lipid Bilayer: Insights from Dual-Resolution Molecular Dynamics. *Soft Matter* **2010**, *6*, 3797–3808.
- (6) Lúcio, M.; Lima, J. L. F. C.; Reis, S. Drug–Membrane Interactions: Significance for Medicinal Chemistry. *Curr. Med. Chem.* **2010**, *17*, 1795–1809.
- (7) Yamamoto, H.; Liljestrand, H. M. Partitioning of Selected Estrogenic Compounds Between Synthetic Membrane Vesicles and Water: Effects of Lipid Components. *Environ. Sci. Technol.* **2004**, *38*, 1139–1147.
- (8) Seddon, A. M.; Casey, D.; Law, R. V.; Gee, A.; Templer, R. H.; Ces, O. Drug Interactions with Lipid Membranes. *Chem. Soc. Rev.* **2009**, *38*, 2509–2519.
- (9) Seydel, J. K.; Wiese, M. In *Drug–Membrane Interactions: Analysis, Drug Distribution, Modeling*; Mannhold, R., Kubinyi, H., Folkers, G., Eds.; Wiley-VCH Verlag GmbH: Weinheim, Germany, 2002; Vol. 4.
- (10) Grassi, M.; Lapasin, R.; Grassi, G.; Colombo, I. *Understanding Drug Release and Absorption Mechanisms: A Physical and Mathematical Approach*; CRC Press: Boca Raton, FL, 2006.
- (11) Vaes, W. H.; Ramos, E. U.; Hamwijk, C.; Van Holsteijn, I.; Blaauboer, B. J.; Seinen, W.; Verhaar, H. J.; Hermens, J. L. Solid Phase Microextraction as a Tool to Determine Membrane/Water Partition Coefficients and Bioavailable Concentrations in In Vitro Systems. *Chem. Res. Toxicol.* **1997**, *10*, 1067–1072.
- (12) Endo, S.; Escher, B. I.; Goss, K.-U. Capacities of Membrane Lipids to Accumulate Neutral Organic Chemicals. *Environ. Sci. Technol.* **2011**, *45*, 5912–5921.
- (13) Janůšová, B.; Skolová, B.; Tůkřová, K.; Wojnarová, L.; Šimůnek, T.; Mladěnka, P.; Filipický, T.; Ríha, M.; Roh, J.; Palát, K.; et al. Amino Acid Derivatives as Transdermal Permeation Enhancers. *J. Controlled Release* **2013**, *165*, 91–100.
- (14) Ingram, T.; Storm, S.; Kloss, L.; Mehling, T.; Jakobtorweihen, S.; Smirnova, I. V. Prediction of Micelle/Water and Liposome/Water Partition Coefficients Based on Molecular Dynamics Simulations, COSMO-RS and COSMOmic. *Langmuir* **2013**, *29*, 3527–3537.
- (15) Vácha, R.; Martínez-Veracoechea, F. J.; Frenkel, D. Intracellular Release of Endocytosed Nanoparticles upon a Change of Ligand–Receptor Interaction. *ACS Nano* **2012**, *6*, 10598–10605.

- (16) Bemporad, D.; Luttmann, C.; Essex, J. W. Computer Simulation of Small Molecule Permeation Across a Lipid Bilayer: Dependence on Bilayer Properties and Solute Volume, Size, and Cross-Sectional Area. *Biophys. J.* **2004**, *87*, 1–13.
- (17) Marrink, S. J.; Berendsen, H. J. C. Permeation Process of Small Molecules Across Lipid Membranes Studied by Molecular Dynamics Simulations. *J. Phys. Chem.* **1996**, *100*, 16729–16738.
- (18) Neale, C.; Bennett, W. F. D.; Tieleman, D. P.; Pomès, R. Statistical Convergence of Equilibrium Properties in Simulations of Molecular Solutes Embedded in Lipid Bilayers. *J. Chem. Theory Comput.* **2011**, *7*, 4175–4188.
- (19) Orsi, M.; Sanderson, W. E.; Essex, J. W. Permeability of Small Molecules through a Lipid Bilayer: A Multiscale Simulation Study. *J. Phys. Chem. B* **2009**, *113*, 12019–12029.
- (20) Jämbeck, J. P. M.; Lyubartsev, A. P. Implicit Inclusion of Atomic Polarization in Modeling of Partitioning between Water and Lipid Bilayers. *Phys. Chem. Chem. Phys.* **2013**, *15*, 4677–4686.
- (21) Zhang, Y.; Voth, G. A. Combined Metadynamics and Umbrella Sampling Method for the Calculation of Ion Permeation Free Energy Profiles. *J. Chem. Theory Comput.* **2011**, *7*, 2277–2283.
- (22) Lange, O. F.; Schäfer, L. V.; Grubmüller, H. Flooding in GROMACS: Accelerated Barrier Crossings in Molecular Dynamics. *J. Comput. Chem.* **2006**, *27*, 1693–1702.
- (23) Mouritsen, O. G.; Jorgensen, K. A New Look at Lipid–Membrane Structure in Relation to Drug Research. *Pharm. Res.* **1998**, *15*, 1507–1519.
- (24) Nagle, J. F.; Tristram-Nagle, S. Structure of Lipid Bilayers. *Biochim. Biophys. Acta* **2000**, *1469*, 159–195.
- (25) Berka, K.; Palončyová, M.; Anzenbacher, P.; Otyepka, M. Behavior of Human Cytochromes P450 on Lipid Membranes. *J. Phys. Chem. B* **2013**, *117*, 11556–11564.
- (26) Taylor, J.; Whiteford, N. E.; Bradley, G.; Watson, G. W. Validation of All-Atom Phosphatidylcholine Lipid Force Fields in the Tensionless NPT Ensemble. *Biochim. Biophys. Acta* **2009**, *1788*, 638–649.
- (27) Siu, S.; Vácha, R.; Jungwirth, P.; Böckmann, R. A. Biomolecular Simulation of Membranes: Physical Properties from Different Force Fields. *J. Chem. Phys.* **2008**, *128*, 125103.
- (28) Prakash, P.; Sankaramakrishnan, R. Force Field Dependence of Phospholipid Headgroup and Acyl Chain Properties: Comparative Molecular Dynamics Simulations of DMPC Bilayers. *J. Comput. Chem.* **2010**, *31*, 266–277.
- (29) Piggot, T. J.; Piñeiro, Á.; Khalid, S. Molecular Dynamics Simulations of Phosphatidylcholine Membranes: A Comparative Force Field Study. *J. Chem. Theory Comput.* **2012**, *8*, 4593–4609.
- (30) Palončyová, M.; Berka, K.; Otyepka, M. Convergence of Free Energy Profile of Coumarin in Lipid Bilayer. *J. Chem. Theory Comput.* **2012**, *8*, 1200–1211.
- (31) Jämbeck, J. P. M.; Lyubartsev, A. P. Exploring the Free Energy Landscape of Solutes Embedded in Lipid Bilayers. *J. Phys. Chem. Lett.* **2013**, *4*, 1781–1787.
- (32) Tomasi, J.; Mennucci, B.; Cammi, R. Quantum Mechanical Continuum Solvation Models. *Chem. Rev.* **2005**, *105*, 2999–3093.
- (33) Tomasi, J. Selected Features of the Polarizable Continuum Model for the Representation of Solvation. *Wiley Interdiscip. Rev.: Comput. Mol. Sci.* **2011**, *1*, 855–867.
- (34) Klamt, A.; Huniar, U.; Spycher, S.; Keldenich, J. COSMOmic: A Mechanistic Approach to the Calculation of Membrane–Water Partition Coefficients and Internal Distributions within Membranes and Micelles. *J. Phys. Chem. B* **2008**, *112*, 12148–12157.
- (35) Jakobtorweihen, S.; Ingram, T.; Smirnova, I. Combination of COSMOmic and Molecular Dynamics Simulations for the Calculation of Membrane–Water Partition Coefficients. *J. Comput. Chem.* **2013**, *34*, 1332–1340.
- (36) Buggert, M.; Cadena, C.; Mokrushina, L.; Smirnova, I.; Maginn, E. J.; Arlt, W. COSMO-RS Calculations of Partition Coefficients: Different Tools for Conformation Search. *Chem. Eng. Technol.* **2009**, *32*, 977–986.
- (37) Domański, J.; Stansfeld, P. J.; Sansom, M. S. P.; Beckstein, O. Lipidbook: A Public Repository for Force-Field Parameters Used in Membrane Simulations. *J. Membr. Biol.* **2010**, *236*, 255–258.
- (38) Berger, O.; Edholm, O.; Jahnig, F. Molecular Dynamics Simulations of a Fluid Bilayer of Dipalmitoylphosphatidylcholine at Full Hydration, Constant Pressure and Constant Temperature. *Biophys. J.* **1997**, *72*, 2002–2013.
- (39) Schüttelkopf, A. W.; Van Aalten, D. M. F. PRODRG: A Tool for High-Throughput Crystallography of Protein–Ligand Complexes. *Acta Crystallogr., Sect. D* **2004**, *60*, 1355–1363.
- (40) Cieplak, P.; Caldwell, J.; Kollman, P. Molecular Mechanical Models for Organic and Biological Systems Going beyond the Atom Centered Two Body Additive Approximation: Aqueous Solution Free Energies of Methanol and *N*-Methyl Acetamide, Nucleic Acid Base, and Amide Hydrogen Bonding and Chloroform/Water Partition Coefficients of the Nucleic Acid Bases. *J. Comput. Chem.* **2001**, *22*, 1048–1057.
- (41) Lemkul, J. A.; Allen, W. J.; Bevan, D. R. Practical Considerations for Guiding GROMOS-Compatible Small-Molecule Topologies. *J. Chem. Inf. Model.* **2010**, *50*, 2221–2235.
- (42) Frisch, M. J.; Trucks, G. W.; Schlegel, H. B.; Scuseria, G. E.; Robb, M. A.; Cheeseman, J. R.; Montgomery, J. A., Jr.; Vreven, T.; Kudin, K. N.; Burant, J. C. et al. *Gaussian 03*, revision E.01; Gaussian, Inc.: Wallingford, CT, 2004.
- (43) Case, D. A.; Darden, T. A.; Cheatham, T. E., III; Simmerling, C. L.; Wang, J.; Duke, R. E.; Luo, R.; Walker, R. C.; Zhang, W.; Merz, K. M.; et al. *AMBER 11*; University of California: San Francisco, CA, 2010.
- (44) Palončyová, M.; Berka, K.; Otyepka, M. Molecular Insight into Affinities of Drugs and Their Metabolites to Lipid Bilayers. *J. Phys. Chem. B* **2013**, *117*, 2403–2410.
- (45) Košinová, P.; Berka, K.; Wykes, M.; Otyepka, M.; Trouillas, P. Positioning of Antioxidant Quercetin and its Metabolites in Lipid Bilayer Membranes: Implication for Their Lipid- Peroxidation Inhibition. *J. Phys. Chem. B* **2012**, *116*, 1309–1318.
- (46) Becke, A. D. Density-Functional Exchange-Energy Approximation with Correct Asymptotic Behavior. *Phys. Rev. A* **1988**, *38*, 3098–3100.
- (47) Perdew, J. P. Density-Functional Approximation for the Correlation Energy of the Inhomogeneous Electron Gas. *Phys. Rev. B* **1986**, *34*, 7406.
- (48) Klamt, A. *COSMO-RS: From Quantum Chemistry to Fluid Phase Thermodynamics and Drug Design*; Elsevier Science Ltd.: Amsterdam, The Netherlands, 2005.
- (49) Bennett, C. Efficient Estimation of Free Energy Differences from Monte-Carlo Data. *J. Comput. Phys.* **1976**, *22*, 245–268.
- (50) Berendsen, H. J. C.; Grigera, J. R.; Straatsma, T. P. The Missing Term in Effective Pair Potentials. *J. Phys. Chem.* **1987**, *91*, 6269–6271.
- (51) MacCallum, J. L.; Bennett, W. F. D.; Tieleman, D. P. Distribution of Amino Acids in a Lipid Bilayer from Computer Simulations. *Biophys. J.* **2008**, *94*, 3393–3404.
- (52) Tristram-Nagle, S.; Nagle, J. F. Lipid Bilayers: Thermodynamics, Structure, Fluctuations, and Interactions. *Chem. Phys. Lipids* **2004**, *127*, 3–14.
- (53) Afri, M.; Gottlieb, H. E.; Frimer, A. A. Superoxide Organic Chemistry within the Liposomal Bilayer, Part II: A Correlation between Location and Chemistry. *Free Radical Biol. Med.* **2002**, *32*, 605–618.
- (54) Vazdar, M.; Jurkiewicz, P.; Hof, M.; Jungwirth, P.; Cwiklik, L. Behavior of 4-Hydroxynonenal in Phospholipid Membranes. *J. Phys. Chem. B* **2012**, *116*, 6411–6415.
- (55) Nitschke, W. K.; Vequi-Suplicy, C. C.; Coutinho, K.; Stassen, H. Molecular Dynamics Investigations of PRODAN in a DLPC Bilayer. *J. Phys. Chem. B* **2012**, *116*, 2713–2721.
- (56) Marrink, S.-J.; Berendsen, H. J. C. Simulation of Water Transport through a Lipid Membrane. *J. Phys. Chem.* **1994**, *98*, 4155–4168.

(57) Oostenbrink, C.; Soares, T. A.; Van der Vegt, N. F. A.; Van Gunsteren, W. F. Validation of the 53A6 GROMOS Force Field. *Eur. Biophys. J.* **2005**, *34*, 273–284.